Thermal, dielectric and barocaloric properties in NH_4HSO_4 crystallized from an aqueous solution and the melt

E.A. Mikhaleva[1,*], I.N. Flerov[1,2], A.V. Kartashev[1,3], M.V. Gorev[1,2], E.V. Bogdanov[1,4], V.S. Bondarev[1,2]

[1]Kirensky Institute of Physics, Federal Research Center KSC SB RAS, 660036, Krasnoyarsk, Russia

[2]Siberian Federal University, 660074 Krasnoyarsk, Russia

[3]Astafijev Krasnoyarsk State Pedagogical University, 660049 Krasnoyarsk, Russia

[4]Krasnoyarsk State Agrarian University, 660049 Krasnoyarsk, Russia

* Corresponding author E.A. Mikhaleva

E-mail address: katerina@iph.krasn.ru

e-mail: katerina@iph.krasn.ru (E.A. Mikhaleva), flerov@iph.krasn.ru (I.N. Flerov), akartashev@yandex.ru (A.V. Kartashev), gorev@iph.krasn.ru (M.V. Gorev), evbogdanov@iph.krasn.ru (E.V. Bogdanov), vbondarev@yandex.ru (V.S. Bondarev)

Abstract

The study of heat capacity, thermal dilatation, permittivity, dielectric loops and susceptibility to hydrostatic pressure was carried out on the quasi-ceramic samples of NH_4HSO_4 obtained from an aqueous solution as well as the melt. The main parameters of the successive $P2_1/c$ (T_1) ↔ Pc (T_2) ↔ $P1$ phase transitions do not depend on the method of preparation of samples and close to those determined in previous studies on single crystal and powder except the sign and magnitude of the baric coefficient for T_2.

Direct measurements of pressure effect on permittivity and thermal properties showed dT_2/dp = - 123 K·GPa^{-1} which is consistent well in magnitude and sign with the baric coefficient evaluated using dilatometric and calorimetric data in the framework of the Clausius-Clapeyron equation. Thus, the temperature region of the ferroelectric *Pc* phase existence extends under pressure. Strong decrease in the entropy jump at the $Pc \leftrightarrow P1$ transformation with pressure increase as well as linear dependence of T_2 against pressure lead one to conclude that pressure shifts this phase transition towards the tricritical point on T - p phase diagram. Significant barocaloric effect was found in the region of the $Pc \leftrightarrow P1$ phase transition.

Keywords Ferroelectric, Phase transition, Thermal and dielectric properties, Entropy, Phase diagram

1. Introduction

In spite the fact, that ferroelectric properties in ammonium hydrogen sulfate, NH_4HSO_4, were found many years ago [1] and actively studied, this compound remains still in the interests of investigators. The most important peculiarities of NH_4HSO_4 are associated, first, with the existence of spontaneous polarization in the restricted temperature range between T_1 = 270 K and T_2 = 154 K [1], second, with piezoelectric properties existed below T_1 and T_2 at least down to 77 K [1], third, with a possibility to be grown from the melt as well as an aqueous solution [2], fourth, with T-p phase diagram rich of pressure induced phases [3-5]. The crystal structure and mechanism of structural distortions in ammonium hydrogen sulfate were repeatedly discussed using the results of X-ray, neutron, NMR and Raman scattering investigations [1, 5-9]. The

main conclusions of these studies can be formulated as follows. Successive phase transitions in NH_4HSO_4 are associated with the symmetry lowering $P2_1/c$ (T_1) ↔ Pc (T_2) ↔ $P1$ (in all phases $Z = 8$) upon cooling and belong to the order-disorder transformations. At temperature above T_1, there are two kinds of crystallographically nonequivalent HSO_4^- ions of which one is orientationally disordered between two sites and other is ordered. Below T_1 as well as T_2 all the sulfate groups are completely ordered. Thus, the entropy change associated with the $P2_1/c$ ↔ Pc transformation can be presented as $\Delta S_1 = R \frac{1}{2} \ln 2 = 2.9$ J·(mol·K)$^{-1}$, which is comparable with the experimental values $\Delta S_1 = (1.7 – 2.2)$ J (mol·K)$^{-1}$ [1, 10, 11]. Structural distortion at T_2 is driven by the tilting of the tetrahedra NH_4^+ as well as the large changes in S – O stretching and bending vibrational modes [8, 9]. Such a solely qualitative characterization of the mechanism of the symmetry change does not allow one to calculate simply the entropy change at the Pc ↔ $P1$ phase transition. However, the large value $\Delta S_2 = (6.7 – 8.8)$ J (mol·K)$^{-1}$ found in calorimetric experiments [1, 10] suggests the strong structural changes.

Effect of internal chemical and external pressure on the phase transition temperatures T_1 and T_2 were examined by Rb → NH_4 cationic substitution [12, 13] and by studies of dielectric properties under hydrostatic pressure [4, 14]. In the former case, the study of the $(NH_4)_{1-x}Rb_xHSO_4$ solid solutions revealed a strong decrease in T_2 with increase of the rubidium concentration [13]. Compounds with $x \geq 0.33$ undergo only one transformation $P2_1/c$ ↔ Pc at temperature which is rather close to T_1 in NH_4HSO_4. An increase of the hydrostatic pressure induces thinning of the intermediate ferroelectric phase because of strong difference between baric coefficients $dT_1/dp = 140$ K/GPa and

dT_2/dp = 765 K/GPa [4, 14]. At room temperature and $p > 0.15$ GPa the crystal structure of NH_4HSO_4 was supposed as triclinic $P1$.

Since the ionic radius of the rubidium atom exceeds that of ammonium group in spite of coordination number, one could suppose that the Rb → NH_4 substitution should increase the unit cell volume V_{cell} in $P2_1/c$ phase. It is interesting and even strange but there are no strong evidences about the effect of the Rb → NH_4 cationic substitution on the V_{cell} value in the initial paraelectric $P2_1/c$ phase. According to different data, the unit cell volume of NH_4HSO_4 (V_{cell} = (840.6 – 847.6) Å^3) [1, 6, 7, 9]) was determined either less or more than that in $RbHSO_4$ ((838.7 – 844.5) Å^3) [12, 15-17]).

Moreover, since the Rb → NH_4 substitution is accompanied by the strong different relative change in the unit cell parameters: $\Delta a/a$ = - 1.1 %, $\Delta b/b$ = + 1.7 %, $\Delta c/c$ = - 0.6 % [1, 12], the change of internal chemical pressure is not isotropic. Thus, the absence of the $Pc \leftrightarrow P1$ phase transition in $RbHSO_4$ is most likely associated not with the chemical pressure decrease but with the absence of ammonium ion which plays a significant role in the mechanism of related structural distortions in NH_4HSO_4 [8, 9].

We would like also to pay attention on the ratio between the values of V_{cell} at different temperatures in three phases of NH_4HSO_4 [1, 9] (Fig. 1). According to the data on the volume coefficient of the thermal dilatation β measured between T_2 and room temperature [18], the β value changes only a few in this temperature range and the β anomaly at T_1 is rather small. Thus, to a first raw approximation, one can suppose that the $V_{cell}(T)$ dependence is close to the linear behaviour between room temperature and T_2 as it is shown in Fig. 1.

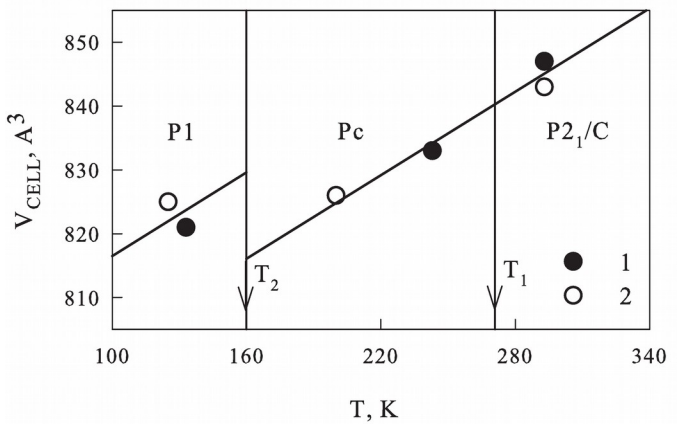

Fig. 1. The ratio between the unit cell volumes V_{cell} in three phases of NH_4HSO_4.
1 - [1], 2 - [9].

The average β values obtained from Fig. 1 (~ $2.5 \cdot 10^{-4}$ K^{-1}) and experimentally determined in [18] ($2 \cdot 10^{-4}$ K^{-1}) are close to each other. Far below phase transition $Pc \leftrightarrow P1$ (T_2 – 30 K), the experimentally found V_{cell} remains close to the value at 200 K [1, 9] and exceeds V_{cell} at T_2 obtained by the linear extrapolation of the $V_{cell}(T)$ dependence from Pc phase. Anyway Fig. 1 clearly shows that at T_2 the volume of NH_4HSO_4 should decrease upon heating from the $P1$ phase to Pc one. Below T_2 the character of the V_{cell} change with temperature was chosen as the same for $T > T_2$. Since the entropy increases with temperature increase $S_{Pc} > S_{P1}$ at the $P1 \leftrightarrow Pc$ phase transition, the baric coefficient in accordance with the Clausius-Clapeyron equation, $dT_2/dp = \delta V/\delta S$, should be negative. It means that the hydrostatic pressure stabilizes ferroelectric phase Pc leading to the expansion of the temperature interval of its existence. It is very strange but the authors [4, 14] did not pay attention to the contradiction between this fact and positive sign of dT_2/dp presented in their papers.

Because we are intended to explore in the future the effect of restricted geometry on the properties of NH_4HSO_4 embedded from the melt into nanoporous boron-silicate glass matrices, it was necessary to have the reliable information on the properties

including the susceptibility to hydrostatic pressure of "free" bulk ferroelectric sample. On the one hand, embedding from the melt allows one to obtain high filling degree, on the other, as far as we know, all previous studies of ammonium hydrosulfate were performed mainly on the samples prepared from an aqueous solution. Therefore, in this work, two types of the polycrystalline NH_4HSO_4 samples were examined: first was crystallized from an aqueous solution and second was obtained after melting the first sample. Hereinafter the samples will be labeled as AHS Sol and AHS Melt, respectively.

2. Experimental

Small single crystals of AHS Sol were obtained by slow evaporation at 45°C from aqueous solution containing equimolar quantities of $(NH_4)_2SO_4$ and H_2SO_4. The AHS Melt sample was prepared by melting at about 160°C the compound synthesized from a water solution.

The quality of both samples used for the experiments was checked at room temperature by XRD which revealed a monoclinic symmetry (sp. gr. $P2_1/c$, $Z = 8$), consistent with suggested in [1, 6, 7, 9]. No additional phases were observed in the samples. Fig. 2 shows the results of Rietveld refinement for the sample AHS Melt.

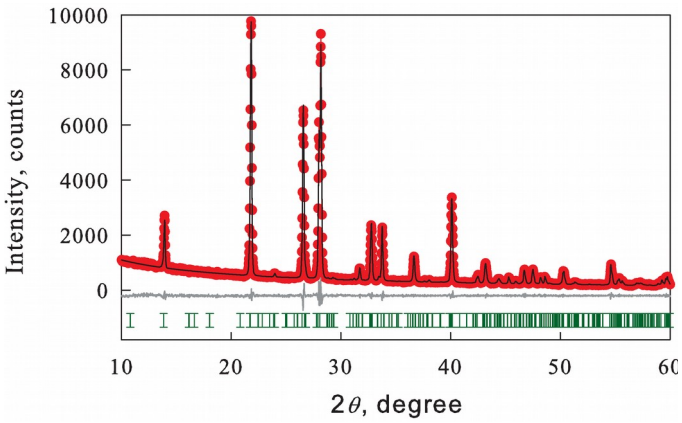

Fig. 2. Difference Rietveld plot of AHS Melt.

The unit cell parameters in this sample (a = 14.3954(7) Å, b = 4.5938(2) Å, c = 14.8343(8) Å, β = 120.883(2) grad) agree with those determined in [1, 9].

All measurements were performed on the same samples prepared as quasi-ceramic disk-shaped pellets of 8 mm diameter and 1.3 mm thickness using uniaxial pressing powdered AHS Sol and AHS Melt without heat treatments because of the presence of ammonium ions. For dielectric measurements, silver electrodes were painted onto the pellet's surface.

On the first stage, thermal dilatation was studied in a temperature range from 100 to 350 K with a heating rate of 3 K/min using a NETZSCH model DIL-402C pushrod dilatometer. Measurements were performed in a dry He flux. Own thermal expansion of the system was taken into account using the results of calibration carried out with quartz as the standard reference. The uncertainty in thermal expansion measurements was about 5 %.

The temperature evolution of the heat capacity $C_p(T)$ of both samples was recorded in a wide temperature range of 80 - 290 K by means of a homemade adiabatic calorimeter with the uncertainty in C_p determination less than 0.5–1.0% [19]. Continuous as well as discrete heating was used for measuring the heat capacity of the "sample + heater + contact grease" system. In the former case, the system was heated at rates of $dT/dt \approx 0.15$–0.30 K/min and in the latter case, the calorimetric step was varied from 1.5 to 3.0 K. The heat capacities of the heater and contact grease were measured in individual experiments.

The dielectric measurements were also carried out in adiabatic calorimeter parallel with heat capacity experiments. The permittivity ε was studied using an E7-20 immittance meter at frequencies from 250 Hz up to 10^6 Hz upon heating at a rate of about 0.5 K/min. The dielectric hysteresis ($P - E$ loops) was examined by an aixACCT EASY CHECK 300 technique. The driving-field profile was a triangular wave of amplitude E_{max}=3 kV/cm. A frequency of measuring electric field was 250 Hz.

The investigations of the susceptibility of the phase transition temperatures in NH_4HSO_4 to hydrostatic pressure were carried out in a piston-cylinder type vessel associated with a pressure multiplier. Pressure up to 0.25 GPa was generated using pentane as the pressure-transmitting medium. Pressure and temperature were measured with manganin gauge and a copper-constantan thermocouple with accuracies of about ± 10^{-3} GPa and ± 0.3 K, respectively.

Because the phase transition at T_2 is of a first order accompanied by large entropy change and reliably detected stepwise change in permittivity [1, 10], we determined the baric coefficient dT_2/dp by measuring both permittivity and differential thermal analysis (DTA) signal. In the latter case, a sample was glued onto one of two junctions of germanium-copper thermocouple characterized by high sensitivity to the temperature change. Quartz sample cemented to the other junction was used as a reference substance. To ensure the reliability of the results, the measurements were performed for both increasing and decreasing pressure cycles.

High temperature transformation is of a typical second order with rather small change of heat capacity at T_1 [1, 10]. Therefore measurements of dT_1/dp were performed mainly by the detecting the shift of large anomaly in permittivity under pressure.

Error bars on all experimental and calculated data were determined taking into account the uncertainty in the basic quantities (temperature, pressure, heat capacity, thermal expansion) measurement.

3. Results and discussion

The results of dilatometric studies presented in Fig. 3 show that the temperature evolution of the linear strain $\Delta L/L_0$ is the same for AHS Sol and AHS Melt.

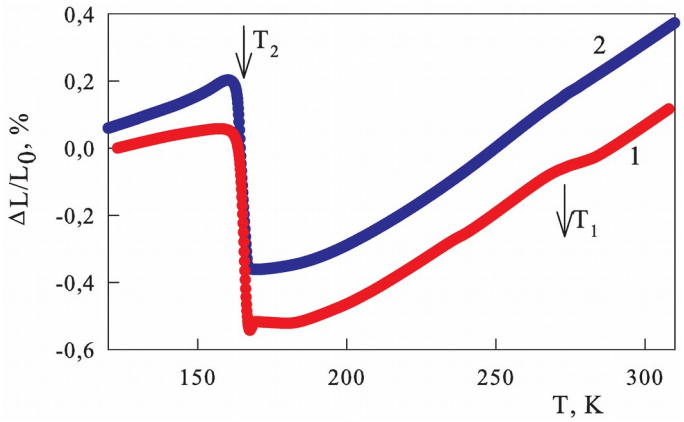

Fig. 3. Temperature dependence of the linear strain in AHS Sol (1) and AHS Melt (2).

Second order phase transition at $T_1 = 273 \pm 2$ K was detected as a small deviation from monotonous increase of $\Delta L/L_0$ with temperature elevating. In accordance with the first order $P1 \leftrightarrow Pc$ transformation, strong anomalous behaviour in the linear strain was observed in the narrow temperature range around T_2. The values of both temperature $T_2 = 165.5 \pm 1$ K and negative strain jump $\delta(\Delta L/ L_0)_{T=T2} = -(0.50 \pm 0.02)$ % were found the same for both samples. The volume strain change for quasi-ceramic samples was determined as $\delta(\Delta V/V_0)_{T=T2} = 3\delta(\Delta L/ L_0)_{T=T2} = -(1.50 \pm 0.07)$ %. This value gives the dominant contribution to the total change in the volume strain $\delta(\Delta V/V_0)_{T=T2}/\Delta(\Delta V/V_0) = 0.87 \pm 0.05$ clearly indicating that the $P1 \leftrightarrow Pc$ phase

transition is far from the tricritical point where $\delta(\Delta V/V_0) \rightarrow 0$. The results obtained agree well with those presented in [1, 9] and Fig. 1 showing that the volume of NH_4HSO_4 decreases upon heating through the $P1 \leftrightarrow Pc$ transformation. This means that in accordance with the Clausius-Clapeyron equation, hydrostatic pressure should decrease the temperature T_2 contrary to its increase associated with the large positive baric coefficient dT_2/dp proposed in previous experiments [4, 14]. It is interesting to point out that the negative change upon heating was also found in the linear strain along ferroelectric *c* axis of the NH_4HSO_4 single crystal [10].

The data obtained by adiabatic calorimeter are shown in Fig. 4a. Two heat capacity anomalies were observed at temperatures $T_1 = 270.5 \pm 0.5$ K and $T_2 = 159 \pm 0.5$ K which are a little bit lower than those determined in dilatometric measurements because in the latter case the rate of the temperature variation was higher. On the other hand, both phase transition temperatures agree well with determined in heat capacity measurements on single crystal of NH_4HSO_4 [10].

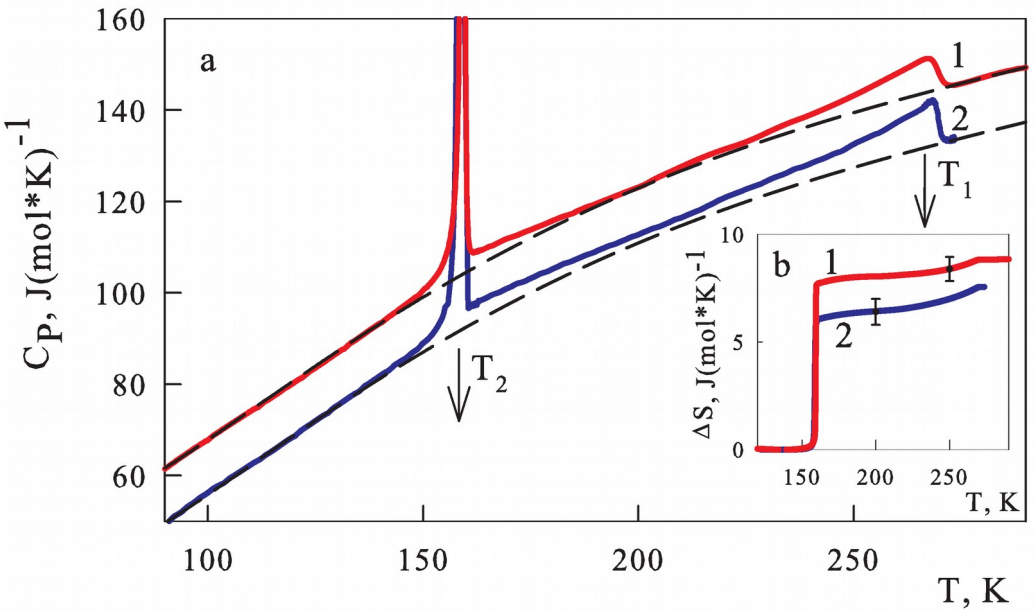

Fig. 4. (a) Temperature dependences of the molar heat capacity of AHS Sol (1) and AHS Melt (Curve 2 is shifted down at 12 J(mol K)$^{-1}$. Dashed line is the lattice heat capacity.

(b) Temperature dependences of the excess entropy associated with the $P2_1/c \leftrightarrow Pc \leftrightarrow P1$ phase transitions.

As it was observed in dilatometric measurements, calorimetric experiments also revealed a small stepwise anomaly at T_1 characteristic for the second order transition and very large peak of the heat capacity at T_2 associated mainly with the enthalpy (entropy) jump at a strong first order phase transformation.

In order to get information on integral thermodynamic characteristics of phase transitions such as enthalpy and entropy changes, separation of the lattice, C_{lat}, and anomalous, ΔC_p, parts of the total heat capacity, C_p, was performed by fitting the experimental data taken far from the transitions points ($T < 145$ K and $T > 272$ K) using equation $C_{lat} = a + bT + cT^2 + dT^3 + eT^{-2}$. The average deviation of the experimental data from the smoothed curves does not exceed 0.5 %. The lattice contribution is shown as a dashed line in Fig. 4a. It is seen that at T_1 the smearing of ΔC_p associated with ceramic nature of the samples was observed only in a narrow temperature interval $T_1 + 3$ K. In the *Pc* phase anomalous contribution ΔC_p exists far below T_1 in accordance with the behaviour of polarization $\Delta C_p \sim (\partial \Delta S/\partial T)_p \sim (\partial P^2/\partial T)_p$ [1, 10].

By integration of the $\Delta C_p(T)$ function the enthalpy of phase transitions were determined: AHS Sol - $\Delta H_1 = 195 \pm 20$ J·mol^{-1} and $\Delta H_2 = 1280 \pm 130$ J·mol^{-1}; AHS Melt - $\Delta H_1 = 270 \pm 40$ J·mol^{-1} and $\Delta H_2 = 1050 \pm 100$ J·mol^{-1} .

Figure 4b shows the temperature behaviour of excess entropy associated with the successive phase transitions in both AHS Sol and AHS Melt, which was calculated by integration of the area below the $\Delta C_p/T$ versus T curves. It seen that there is a difference between two curves. However, taking into account the uncertainty of heat capacity measurements as well as choosing C_{lat}, the values of entropy changes are close to each

other (AHS Sol - $\Delta S_1 = 0.85 \pm 0.08$ J·(mol·K)$^{-1}$, $\Delta S_2 = 8.0 \pm 1.0$ J·(mol·K)$^{-1}$; AHS Melt - $\Delta S_1 = 1.19 \pm 0.15$ J·(mol·K)$^{-1}$, $\Delta S_2 = 6.5 \pm 0.7$ J·(mol·K)$^{-1}$,) and comparable with entropies determined for single crystal of NH_4HSO_4 ($\Delta S_1 = 1.66 \pm 0.20$ J·(mol·K)$^{-1}$, $\Delta S_2 = 6.7 \pm 0.7$ J·(mol·K)$^{-1}$) [10]. The ratio between the jump δS_2 (AHS Sol – 7.5 ± 0.5 J·(mol·K)$^{-1}$; AHS Melt – 6.0 ± 0.5 J·(mol·K)$^{-1}$) and the total change in the entropy $\delta S_2/\Delta S_2 \approx 0.93$ is close to $\delta(\Delta V/V_0)_{T=T2}/\Delta(\Delta V/V_0)$ value shown above and can be considered as an additional evidence for significant distance of the first order $Pc \leftrightarrow P1$ phase transition from the tricritical point.

The permittivity in the quasi-ceramic sample AHS Melt (Fig. 5a, b) exhibits specific features identical to those observed in the $\varepsilon(T)$ dependence for the single-crystal sample [1, 20]: a jump at $T_2 = 161 \pm 1$ K and a pronounced peak at $T_1 = 271.4 \pm 0.5$ K. At low frequency $f = 250$ Hz , a strong increase of ε was observed above ~ 190 K from 13 up to 250 at 290 K, which was diminished with the increase in f up to 1 MHz.

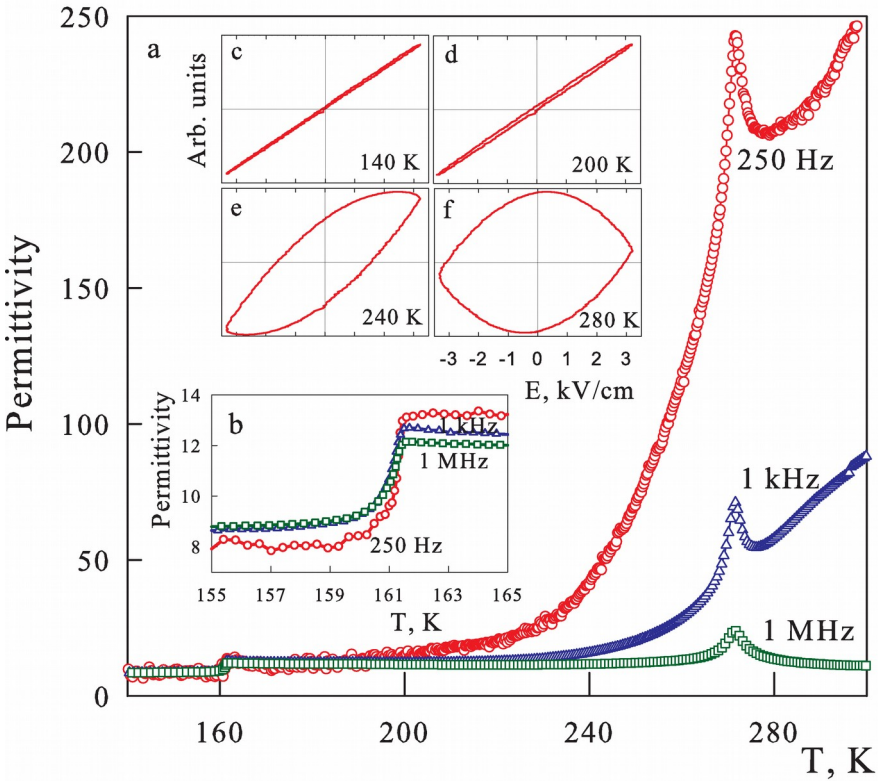

Fig. 5. (a, b) Dependences of permittivity on temperature for AHS Melt at different frequencies. (c, d, e, f) Dielectric hysteresis loops at the corresponding temperatures.

The behaviour of the ε peak at T_1 and stepwise change at T_2 was also changed but to significantly lesser extent. The temperatures of both phase transitions were not affected by the frequency variation and agree well with those found in calorimetric measurements.

We performed also examination of the $P - E$ loops in three phases. As example, the results on AHS Melt are shown in Fig. 5c, d, e, f, which confirm that the polarization is not the best property to study the effect of hydrostatic pressure on the temperature T_2, as it was also demonstrated on single crystal of NH_4HSO_4 in [14]. First, it was found that there is rather strong relaxation in the appearance of P in the Pc phase: almost linear dependence of polarization versus electric field exists far above T_2 (Fig. 5c, d). Second, the "non-classic" shaped dielectric loops does not allows one the correct determination of polarization. The latter circumstance can be associated with the low density of the quasi-ceramic samples prepared without heat treatments as well as the high electrical conductivity observed in [21]. Both factors can contribute for the quasi-ceramic sample; however, the main role is most likely played by the last factor.

The results of the hydrostatic pressure effect on the permittivity of both NH_4HSO_4 samples at the phase transitions $P2_1/c \leftrightarrow Pc \leftrightarrow P1$ were found similar. The experimental data for AHS Melt are presented in Fig. 6.

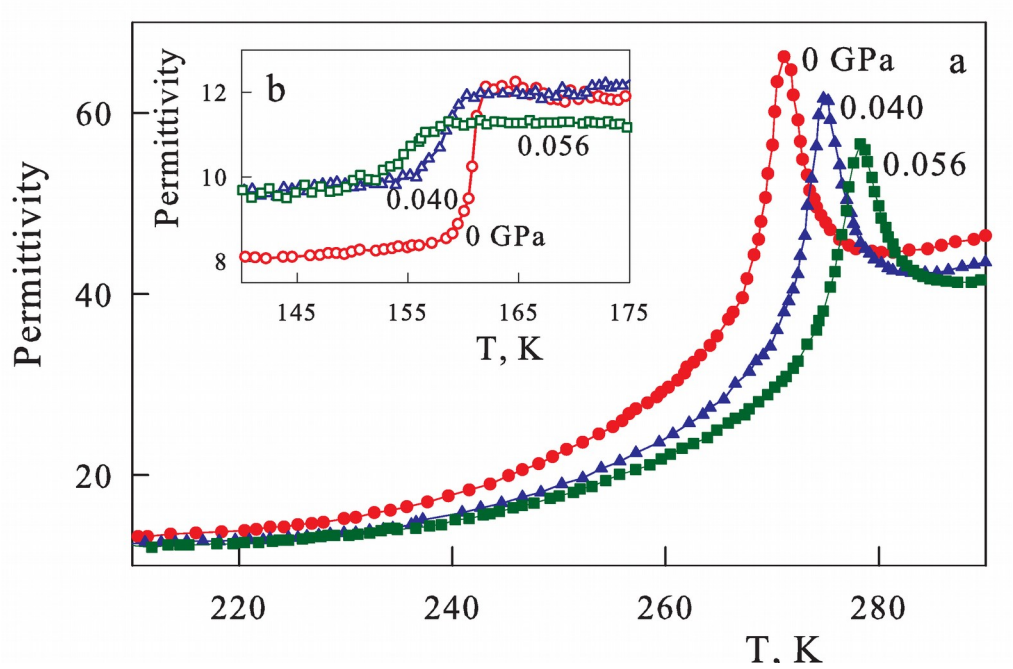

Fig. 6. Temperature dependence of permittivity for AHS Melt measured upon heating at different pressures around $P2_1/c \leftrightarrow Pc$ (a) and $Pc \leftrightarrow P1$ (b) phase transitions.

The temperature behaviour of permittivity in the region of T_1 is similar to that observed in [4, 14]: the permittivity peak shifts under pressure to higher temperature and decreases in the maximum value (Fig. 6a). The corresponding baric coefficient $dT_1/dp = 90 \pm 15$ K·GPa^{-1} is close to measured in [4, 14] and calculated in [18].

As to the $\varepsilon(T, p)$ data around $Pc \leftrightarrow P1$ transformation (Fig. 6b), they showed the decrease in T_2 accompanied by the smearing and diminishing step-wise permittivity anomaly. The observed negative sign of dT_2/dp is in contradiction to increase T_2 with pressure proposed by earlier experiments also studied dielectric properties [4, 14].

Since heat capacity of NH_4HSO_4 demonstrated very large anomaly at low temperature transformation (Fig. 4), we were able to investigate the pressure effect on the DTA signal associated with the heat effect at T_2. These experiments revealed in both AHS Sol and AHS Melt, first, a strong shift in T_2 to lower temperatures and, second, a suppression of the square under DTA(T) curves with pressure increase (Fig. 7a, b).

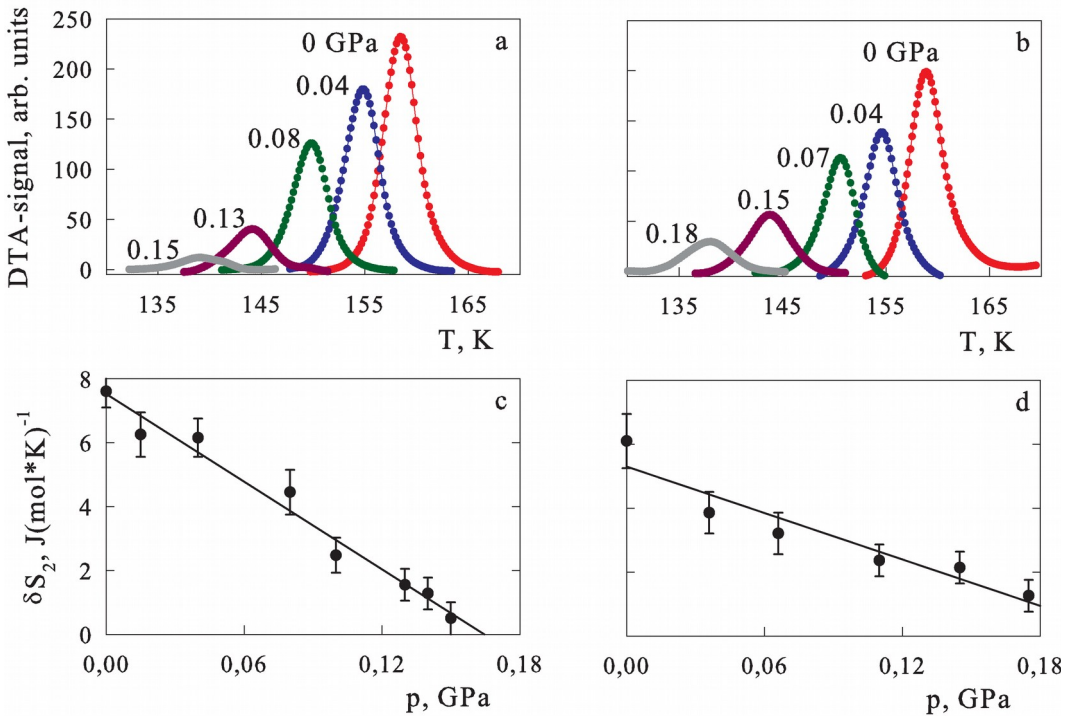

Fig. 7. (a, b) Anomalous component of the DTA signal near T_2 at different pressures in AHS Sol and AHS Melt, respectively. (c, d) Entropy jump δS_2 for the first-order transition in AHS Sol and AHS Melt, respectively, Lines in c and d represent linear fits.

Thus, thermal and dielectric properties of NH_4HSO_4 demonstrate similar behaviour at T_2 under pressure characterized by the negative baric coefficient.

As usual, the DTA measurements allow one to detect the heat effect associated with the latent heat or in other words with enthalpy δH or entropy $\delta S = \delta H/T_{PT}$ jump at the phase transition point T_{PT}. Because the total entropy (as well as enthalpy) change takes place in both samples under study in a very narrow temperature range near T_2, one can suppose that the DTA experiments above show the decrease of δS_2. This process is accompanied at the same time by the appearance of the temperature and pressure dependent part of the excess entropy $\Delta S_2^*(T, p)$ in a certain temperature range, expanding with the pressure. Thus, the total entropy change $\Delta S_2 = \delta S_2(p) + \Delta S_2^*(T, p)$ remains constant in NH_4HSO_4 at least up to $p \leq 0.23$ GPa realized in our measurements (Fig. 7b). This assumption is a realistic because it is difficult to imagine that such a low

pressure can change a degree of disorder of structural elements. Thus, a more reasonable and plausible hypothesis is that the pressure induces the approaching the *Pc* ↔ *P*1 transformation to the tricritical point, which is characterized by $\delta H = 0$ and $\delta S = 0$ [22].

In Fig. 7c, d one can see a linear decrease in the entropy jumps in both samples which are equal to zero at the pressure of the tricritical point $p_{TCP} \approx 0.17$ GPa in AHS Sol and ~ 0.22 GPa in AHS Melt. Taking into account the experimental uncertainties, a difference in the p_{TCP} values for different samples can be considered as insignificant.

The experimental results on the pressure effect on both phase transitions in AHS Sol and AHS Melt obtained by measuring ε and δS_2 are summarized on $T - p$ phase diagram (Fig. 8).

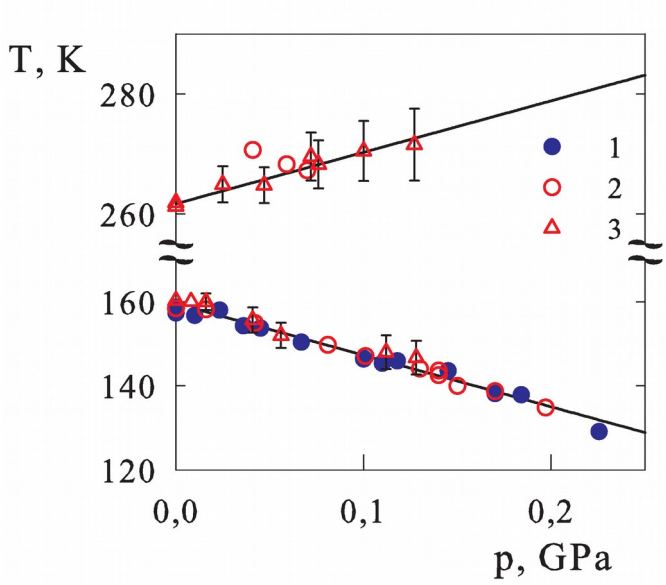

Fig. 8. Temperature – pressure phase diagram combining the results on the DTA signal (1, 2) and permittivity (3) study in AHS Sol (2, 3) and AHS Melt (1).

Both properties of the samples under study show the same pressure dependence of T_2 characterized by the negative baric coefficient $dT_2/dp = -123 \pm 15$ K·GPa^{-1}. A shift of T_2 under pressure was also determined using the results of heat capacity and thermal

dilatation measurements in the framework of the Clausius-Clapeyron equation $dT_2/dp = \delta V_2/\delta S_2$. These values for AHS Sol (-128 ± 16 $K \cdot GPa^{-1}$) and AHS Melt (-158 ± 20 $K \cdot GPa^{-1}$) are close to that obtained in the direct measurements of $T_2(p)$.

Such a good agreement between the data obtained by three independent experiments performed on two samples of NH_4HSO_4 prepared by different methods suggested a high reliability of determination of the dT_2/dp sign and value.

And what could be the reason of the contradiction between these results and data obtained in [4, 14], where the value dT_2/dp was found positive and very large + 765 $K \cdot GPa^{-1}$? We do not think that it is connected with the kind of the sample: single crystal [4, 14] and quasi-ceramics used in the present study. The temperatures and entropies of the phase transitions $P2_1/c \leftrightarrow Pc \leftrightarrow P1$ as well as baric coefficient dT_1/dp in AHS Sol and AHS Melt are in satisfactory agreement with the data obtained on powder [1, 5], single crystal [1, 9, 10, 14, 23] and ceramic [20] samples. On the other hand, the volume strain jump $\delta(\Delta V/V_0)$ at T_2 calculated using the Clausius-Clapeyron equation, baric coefficient dT_2/dp from [4, 14] and δS_2 value determined in the present paper or in [1, 10], is unrealistically gigantic ~ (+ 8 %). And at last, the positive shift of T_2 under pressure [4, 14] is in contradiction with the negative sign of volume strain upon heating through the $P1 \leftrightarrow Pc$ phase transition found by us (Fig. 3) and in [1, 14].

A constancy of the dT_2/dp value in AHS Sol and AHS Melt at least in the range of pressure studied means the fall of δV_2 in accordance with the decrease of δS_2. Similar correlated decrease in the volume and entropy changes with pressure was recently observed in $(NH_4)_2SO_4$ undergoing ferrielectric phase transition of the first order characterized by the negative baric coefficient [24]. It is safe to assume that this transformation is also close to the tricritical point. Of course the fall of δS_2 as well as

δV_2 under pressure is not common peculiarity of phase transitions. For example, recent studies of the $T - p$ phase diagrams in some perovskite-like ferroelastics have shown the constancy of the entropy jump at phase transition point at least in the range of p = 0 – 0.5 GPa [25, 26].

A constant ratio between the values of $\delta S_2(p)$ and $\Delta S_2^*(T, p)$ with the pressure change is very convenient for the analysis of barocaloric effect (BCE) which is associated with the entropy decrease or temperature increase with pressure elevating at T = const or S = const, respectively. However, for detailed and correct determination of BCE in NH_4HSO_4 as well as in recently studied $(NH_4)_2SO_4$ [24], characterized by δS_2 decrease and $\Delta S_2^*(T, p)$ increase with the pressure increase, it is necessary to have information on the pressure dependence of the heat capacity. Owing to a lack of opportunity to measure $C_p(T, p)$, BCE in $(NH_4)_2SO_4$ was evaluated only in connection with the δS_2 part of entropy [24]. We were also not able to determine the $\Delta S_2^*(T, p)$ dependence for NH_4HSO_4. However, taking into account that the maximum value of the extensive BCE ΔS_{BCE}^{max} near T_2 is equal to the phase transition entropy ΔS_2, one can perform raw estimation of the minimum pressure, p_{min}, which produces the maximum values of ΔS_{BCE}^{max} as well as ΔT_{AD}^{max} [26]

$$p_{min} \geq \frac{T\Delta S_2}{C_p dT_2/dp} \qquad \Delta T_{AD}^{max} = \frac{dT_2}{dp} p_{min}$$

Use of the C_p, ΔS_2 and dT_2/dp values determined above for AHS Sol and AHS Melt gives p_{min} = 0.10 ± 0.02 GPa and ΔT_{AD}^{max} = - 12 ± 2 K, which are close to those found for $(NH_4)_2SO_4$ [24]. Negative sign of intensive BCE ($\Delta T_{AD}^{max} < 0$) in both ammonium sulfate and ammonium hydrosulfate (near T_2) is associated with the decrease of the unit cell volume in the region of the phase transition point. On the other hand, both crystals are characterized by the positive volume deformation $\Delta V/V_0 > 0$ far from the transition

temperature, which leads to the conventional BCE ($\Delta S_{BCE} < 0$; $\Delta T_{AD} > 0$) in accordance with the Maxwell equation [27]

$$\left(\frac{\partial S}{\partial p}\right)_T = -\left(\frac{\partial V}{\partial T}\right)_p .$$

This peculiarity will decrease the extensive and intensive inverse BCE in the region of the phase transition. Near the $Pc \leftrightarrow P1$ transformation in NH_4HSO_4, these amendments are – (1.2 ± 0.02) J·(mol·K)$^{-1}$ and + (2.0 ± 0.3 K for ΔS_{BCE} and ΔT_{AD}, respectively.

4. Conclusions

The study of the thermal and dielectric properties performed on two quasi-ceramic samples of NH_4HSO_4 obtained by different ways revealed the following points.

The method of the samples preparation does not affect the main properties associated with the succession of the $P2_1/c$ (T_1) ↔ Pc (T_2) ↔ $P1$ phase transitions. The transformation temperatures, changes of entropy and volume deformation in AHS Sol and AHS Melt are in satisfactory agreement with the data obtained on powder [1, 5], single crystal [1, 9, 10, 14, 23] and ceramic [20] samples.

The direct dilatometric measurements showed the negative change of the volume deformation at T_2 upon heating which coincides with the ratio between unit cell parameters in the Pc and $P1$ phases [1, 9].

The temperature-pressure phase diagram constructed on the ground of the study of susceptibility of DTA signal and permittivity to hydrostatic pressure revealed the expansion of the temperature interval of the ferroelectric phase Pc stability associated with different signs of baric coefficients dT_1/dp and dT_2/dp. The decrease of T_2 under pressure agrees with the negative sign of $\delta(\Delta V/V)_{T=T2}$. The calculated values of baric coefficients are close to obtained in direct measurements.

Pressure increase leads to decrease in the entropy jump δS_2 at the $Pc \leftrightarrow P1$ transformation in AHS Sol and AHS Melt which is connected with approaching of this transformation towards the tricritical point.

The analysis of barocaloric efficiency showed that the maximum extensive and intensive BCE ($\Delta S_{BCE}^{max} = 8 \pm 1$ J(mol·K)$^{-1}$; $\Delta T_{AD}^{max} = 12 \pm 2.0$ K) can be realized at rather low pressure ~ 0.1 GPa. Conventional BCE associated with the $Pc \leftrightarrow P1$ phase transition in NH_4HSO_4 does not exceed ~ 15 % compared to the maximum inverse BCE.

Acknowledgements

We are grateful to T.N. Davydova for preparation of the sample from an aqueous solution and Dr. M.S. Molokeev for X-ray characterization of the samples.

The reported study was partially supported by the Russian Foundation for Basic Research (RFBR), research project No. 16-32-00092 mol_a.

References

[1] R. Pepinsky, K. Vedam, S. Hoshino, Y.S. Okaya, Ammonium hydrogen sulfate: a new ferroelectric with low coercive field, Phys Rev. 111 (1958) 1508–1510.

[2] F. Iona, G. Shirane, Ferroelectric crystals, Pergamon Press, Oxford – London – New York Paris, 1962.

[3] P.W. Bridgman, Polymorphism at high pressures, Proc. Am. Acad. Arts Sci. 52 (1916) 91-187.

[4] K. Gesi, K. Ozawa, Pressure-temperature phase diagram of ferroelectric ammonium bisulfate NH_4HSO_4, J. Phys. Soc Japan 43 (1977) 563-569.

[5] L. Bobrowicz, I. Natkaniec, T. Sarga, S.I. Bragin, Neutron scattering studies of pressure induced phase transitions in NH_4HSO_4, High Pressure Research 14 (1995) 61-65.

[6] R.J. Nelmes, An X-ray diffraction determination of the crystal structure of ammonium hydrosulfate above the ferroelectric transition, Acta Crystallogr. B 27 **(**1971) 272-281.

[7] R.J. Nelmes, The structure of ammonium hydrogen sulfate in its ferroelectric phase and the ferroelectric transition, Ferroelectrics 4 (1972) 133-140.

[8] R. Miller, R. Blinc R., M. Brenman, J.S. Waugh, Nuclear spin-lattice relaxation in some ferroelectric ammonium salts, Phys. Rev. 126 (1962) 528-532.

[9] D. Swain; V.S. Bhadram, P. Chowdhury, C. Narayana, Raman and X-ray Investigations of Ferroelectric Phase Transition in NH_4HSO_4, J. Phys. Chem. A 116 (2012) 223–230.

[10] I.N. Flerov, V.I. Zinenko, L.I.Zherebtsova, I.M. Iskornev, D.Ch. Blat, Study of phase transitions in ammonium hydrosulfate, Izvestiya AN USSR (seriya fizicheskaya) 39 (1975) 752-757.

[11] B.A. Strukov, M.N. Danilycheva, Heat capacity of ammonium hydrogen sulfate in the temperature range between – 7 and + 14 ºC, Fizika Tverdogo. Tela, 5 (1963) 1724-1727.

[12] R. Pepinsky, K. Vedam, Ferroelectric transition in rubidium bisulfate, Phys Rev. 117 (1960) 1502–1503.

[13] E.A. Mikhaleva, I.N. Flerov, V.S. Bondarev, M.V. Gorev, A.D. Vasiliev, T.N. Davydova, Phase transitions and caloric effects in ferroelectric solid solutions of ammonium and rubidium hydrosulfates, Phys. Solid State 53 (2011) 510-517.

[14] I.N. Polandov, V.P. Mylov, B.A: Strukov, On p – T diagram of ferroelectric crystal NH_4HSO_4, Fizika Tverdogo Tela 10 (1968) 2232-2234.

[15] W.G. Mumme, Alkali metal ordering and hydrogen bonding in the system $KHSO_4$-$RbHSO_4$: the crystal structures of $K_xRb_{1-x}HSO_4$ ($0.3 < x < 0.55$) and $RbHSO_4$, Acta Crystallogr. B 29 (1973) 1076-1083.

[16] J.P. Ashmore, H.E. Petch, The structure of $RbHSO_4$ in its paraelectric phase, Can. J. Phys. 53 (1975) 2694-2702.

[17] K. Itoh, H. Ohno, Sh. Kuragaki, Disordered structure of ferroelectric rubidium hydrogen sulfate in the paraelectric phase, J. Phys. Soc. Japan 64 (1995) 479-484.

[18] I.M. Iskornev, I.N. Flerov, Thermal expansion of ferroelectric crystals of the ammonium hydrosulfate family, Fizika Tverdogo Tela 20 (1978) 2649-2653.

[19] A.V. Kartashev, I.N. Flerov, N.V.Volkov, K.A. Sablina, Adiabatic calorimetric study of the intense magnetocaloric effect and the heat capacity of $(La_{0.4}Eu_{0.6})_{0.7}Pb_{0.3}MnO_3$, Phys. Solid State 50 (2008) 2115–2120.

[20] J.E. Diosa, M.E. Fernarndez, R.A. Vargas, Anomalous Phase Behaviour of NH_4HSO_4 below Room Temperature, Phys. Status Sol. (b) 227 (2001) 465–468.

[21] I.N. Flerov, E.A. Mikhaleva, Electrocaloric Effect and Anomalous Conductivity of the Ferroelectric NH_4HSO_4, Phys.Solid State 50 (2008) 478–484.

[22] K.S. Aleksandrov, I.N. Flerov, The region of applicability of thermodynamic theory of structural phase transitions close to tricritical point, Fizika Tverdogo Tela 21 (1979) 327-336.

[23] O. Björkström, A. Fredriksson, B.-E. Mellander, J.E. Diosa, R.A. Vargas, Anomalous behaviour of $(NH_4)HSO_4$, Solid State Ionics 69 (1994)75-77.

[24] P. Lloveras, E. Stern-Taulats, M. Barrio, J.-Ll. Tamarit, S. Crossley, W. Li, V. Pomjakushin, A. Planes, Ll. Mañosa, N.D. Mathur, X. Moya, Giant barocaloric effects at low pressure in ferrielectric ammonium sulphate, Nature communications 6 (2015) 8801 DOI: 10.1038.

[25] I.N. Flerov, M.V. Gorev, A. Tressaud, N.M. Laptash, Perovskite-Like Fluorides and Oxyfluorides: Phase Transitions and Caloric Effects, Crystallography Reports 56 (2011) 9–17.

[26] M.V. Gorev, I.N. Flerov, E.V. Bogdanov, V.N. Voronov, N.M. Laptash, Barocaloric Effect near the Structural Phase Transition in the Rb_2KTiOF_5 Oxyfluoride, Phys. Solid State. 52 (2010) 377–383.

[27] A. M. Tishin, Y. I. Spichkin, The Magnetocaloric Effect and Its Applications, Series in Condensed Matter Physics, Institute of Physics Publ., Bristol, Philadelphia, 2003.